

# Effects of AlGaAs energy barriers on InAs/GaAs quantum dot solar cells

K. A. Sablon,<sup>1,a)</sup> J. W. Little,<sup>1</sup> K. A. Olver,<sup>1</sup> Zh. M. Wang,<sup>2</sup> V. G. Dorogan,<sup>2</sup> Yu. I. Mazur,<sup>2</sup> G. J. Salamo,<sup>2</sup> and F. J. Towner<sup>3</sup>

<sup>1</sup>U.S. Army Research Laboratory, Adelphi, Maryland 20783, USA

<sup>2</sup>Department of Physics, University of Arkansas, Fayetteville, Arkansas 72701, USA

<sup>3</sup>Maxion Technologies, Inc., College Park, Maryland 20740, USA

(Received 1 July 2010; accepted 1 August 2010; published online 13 October 2010)

We have studied the effects of AlGaAs energy barriers surrounding self-assembled InAs quantum dots in a GaAs matrix on the properties of solar cells made with multiple quantum dot layers in the active region of a photodiode. We have compared the fenced dot samples with conventional InAs/GaAs quantum dot solar cells and with GaAs reference cells. We have found that, contrary to theoretical predictions, the AlGaAs fence layers do not enhance the transport properties of photogenerated carriers but instead suppress the extraction of the carriers excited in the dots by light with wavelengths longer than the cutoff wavelength of the GaAs matrix material. Both the standard quantum dots and the fenced dots were found to give solar cell performance comparable to the GaAs reference cells for certain active region thicknesses but neither showed enhancement due to the longer wavelength absorption or improved carrier transport. © 2010 American Institute of Physics. [doi:10.1063/1.3486014]

## I. INTRODUCTION

For decades, several solar cell architectures have been explored for exceeding the Shockley–Queisser limit of efficiency.<sup>1–6</sup> One approach to overcome the efficiency limit of conventional single gap solar cells is the use of low-dimensional semiconductor structures such as quantum dots (QDs) to extend the wavelength response into the near infrared (NIR) region of the solar spectrum.<sup>1,7</sup> A recent theoretical model<sup>8</sup> considered the use of InAs QDs embedded in an AlGaAs high potential barrier fence (known as dots-in-a-fence, or DFENCE) as an approach for improving QD solar cell devices and predicted an energy conversion efficiency in the range of 36% to 45% under 1 sun illumination (100 mw/cm<sup>2</sup>), surpassing that of conventional single-junction solar cells. This predicted enhancement is primarily due to resonant tunneling through new electronic states created by the fence layers and the resulting decrease in trapping and recombination of carriers in the QDs and the wetting layer. To the best of our knowledge, this system has not been studied experimentally. Therefore, in this paper, the optical, structural, and electrical properties of the DFENCE structure will be experimentally explored and compared with conventional InAs/GaAs self-assembled QD solar cells and with standard GaAs solar cells to investigate the influence of the AlGaAs layer on the solar cell parameters.

## II. SAMPLE DESCRIPTION

Single junction GaAs reference, conventional QD and the DFENCE structures were investigated using photoluminescence (PL), spectral response (SR), and current-voltage (I–V) photoresponse measurements. Figure 1 illustrates the growth diagram of a DFENCE QD structure. The structures were grown on n<sup>+</sup> GaAs (100) substrates by molecular beam

epitaxy (MBE). Following oxide desorption, a 300 nm n<sup>+</sup> GaAs buffer with a doping density of 1 × 10<sup>18</sup> cm<sup>-3</sup> was grown at 595 °C. The substrate temperature remained the same during growth of the i-GaAs region of the reference cell but was cooled down to 530 °C for growth of the intrinsic region of the QD solar cell structures. The temperature was increased to 550 °C for the p<sup>+</sup> GaAs and Al<sub>0.45</sub>Ga<sub>0.55</sub>As layers. The DFENCE structure was grown by depositing 1.3 nm of Al<sub>0.2</sub>Ga<sub>0.8</sub>As on either side of the InAs QDs that are formed through the strain driven rearrangement of 2.1 monolayers (MLs) of InAs. The conventional QD structures were grown by depositing 2.1 MLs of InAs directly on GaAs. Structures containing 10, 20, and 40 stacks of QD layers separated by GaAs were grown to determine the dependence of the solar cell parameters on the number of QD layers. The thickness of the separation layer was 50 nm for the 10 and the 20 stack samples and 40 nm for the 40 stack samples. These thicknesses were chosen so that the strain fields associated with the dots (as observed in cross-sectional transmission electron microscope images of calibration samples) were essentially dissipated before the growth of the next layer of dots to prevent strain buildup and eventual dislocation generation. The lower thickness for the 40 stack separation layers was chosen in the interest of minimizing MBE

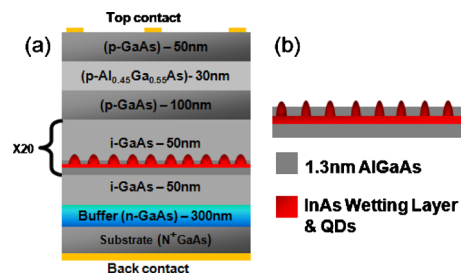


FIG. 1. (Color online) (a) Schematic of the 20 stacked DFENCE and (b) magnified view of the AlGaAs layers on either side of the QDs.

<sup>a)</sup>Electronic mail: k.sablonramsey@us.army.mil.

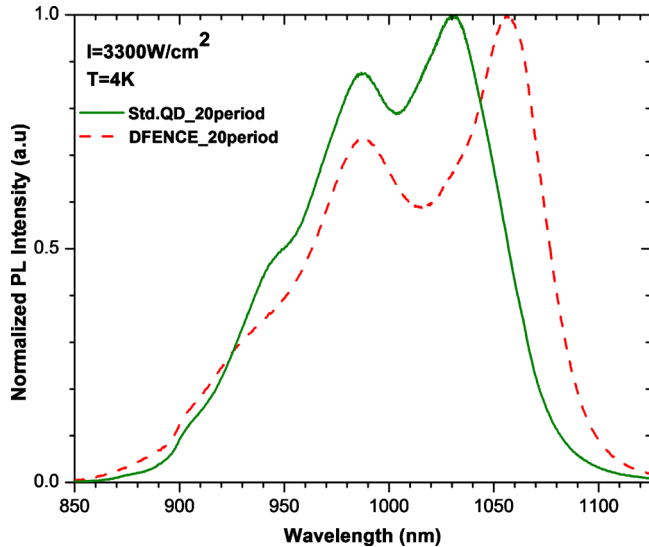


FIG. 2. (Color online) PL measurements at high excitation density for the 20 stack QD structures.

growth time. The GaAs reference cells were grown with uniform GaAs active regions consisting of 500, 1000, and 1600 nm, an equivalent to the overall thicknesses of the 10, 20, and 40 stack InAs QD structures, respectively. The *p-i-n* structure was completed by a 100 nm *p*-GaAs with a doping density of  $1 \times 10^{18} \text{ cm}^{-3}$ , 30 nm *p*-Al<sub>0.45</sub>Ga<sub>0.55</sub>As with a doping density of  $5 \times 10^{18} \text{ cm}^{-3}$ , and finally a 50 nm *p*-GaAs contact layer with a doping density of  $5 \times 10^{18} \text{ cm}^{-3}$ .

### III. LOW TEMPERATURE PL

The normalized PL intensities measured from the unprocessed 20 stack test structure is shown in Fig. 2. The PL measurements were carried out at low temperature ( $T = 10 \text{ K}$ ) in a closed-cycle helium cryostat. For excitation, the 532 nm line from a frequency doubled neodymium doped yttrium aluminum garnet laser was used. The diameter of the laser spot on a sample was  $20 \mu\text{m}$ . The PL signal from the sample was dispersed by a monochromator and detected by an InGaAs detector array. The PL spectra were taken at high

( $3300 \text{ W/cm}^2$ ) excitation density so that luminescence from excited states in the QDs could be observed in addition to that from the ground states. The spectra are normalized independently at the highest intensity peak for each sample. Narrow and well separated peaks are observed for both QD samples. The ground state (longest wavelength) PL peak from the 20 stack DFENCE sample shows a redshift of about 20 meV relative to the conventional QD structure. This shift is most likely due to a combination of a slightly different dot size/shape distribution for the dots grown on AlGaAs (Refs. 9–11) and a suppression of GaAs/InAs intermixing in the dots due to the surrounding AlGaAs layers.<sup>12</sup> Note that both samples show shorter wavelength features of comparable magnitude that are due to luminescence from excited states in the QDs. As will be described in a later section, the small feature at about 900 nm in Fig. 2 plays a substantial role in the photocurrent spectra obtained from diodes fabricated from this material. PL obtained from the 10 stack and the 40 stack wafers (not shown) show similar features to those seen in Fig. 2.

### IV. DEVICE FABRICATION

For I–V and SR characterization,  $250 \mu\text{m}$  circular photodiodes were fabricated using standard photolithography followed by a phosphoric acid wet chemical etch. The structure was etched down into the  $n^+$  GaAs substrate. Subsequently, an *n*-type blanket metallization of gold/tin/gold (15 nm/25 nm/250 nm thicknesses, respectively) was performed in an electron beam vacuum evaporator onto the back side of the substrate. Following blanket metallization, a rapid thermal annealing at  $375 \text{ }^\circ\text{C}$  for 60 s was performed. Finally, the top of each mesa was patterned with a *p*-type metal ring contact. A chromium/gold contact layer (25 nm/250 nm thick, respectively) was deposited followed by a metal liftoff. The contact ring diameter is  $200 \mu\text{m}$  with a  $100 \mu\text{m}$  opening in the center to allow for top-side illumination. An array of these mesas was cleaved from the wafer and mounted in a 68 pin leadless chip carrier (LCC) using indium metal. Wire bonds were attached to the top contact metal and out to a pin connection on the LCC.

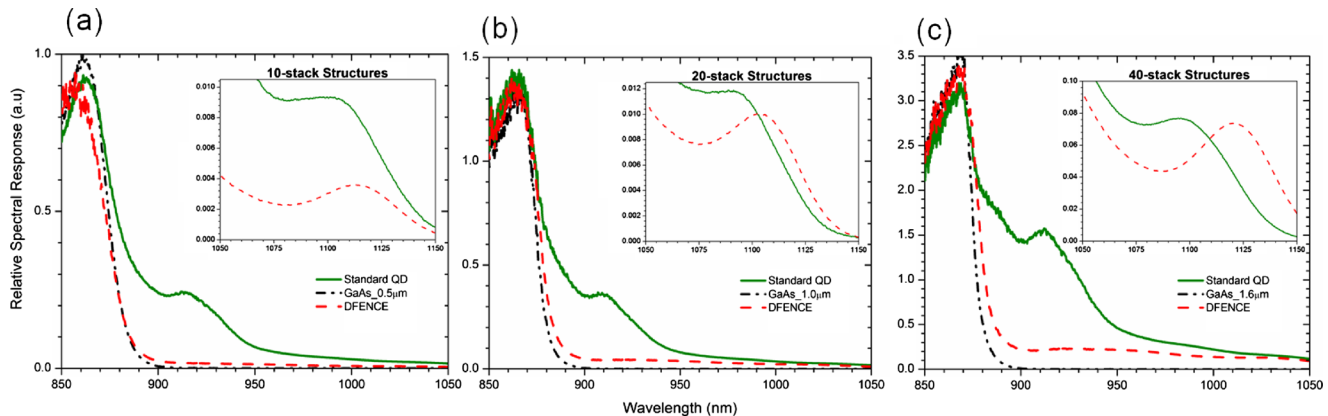


FIG. 3. (Color online) [(a)–(c)] SR of the 10, 20, and 40 stacks QD structures compared with the equivalent GaAs reference cell, respectively. The insets show magnified views of the SR contribution from the QDs.

## V. SR MEASUREMENT

The 300 K spectral photocurrent response measurements were performed with a Nicolet Fourier transform infrared spectrometer and a Keithley 428 current amplifier. The zero-bias spectra for the 10, 20, and 40 stack structures (and equivalent GaAs reference diodes), are shown in Figs. 3(a)–3(c), respectively. Note that there is no photoresponse beyond 900 nm for the GaAs reference cell. However, by incorporating the QDs in the active region, the SR, although relatively weak compared with the GaAs response is extended into the NIR region. The insets in Figs. 3(a)–3(c) show the wavelength region associated with the ground state QD transitions on a magnified scale. While the PL was most intense from these ground state transitions (Fig. 2), the magnitude of the photocurrent associated with them is substantially less than for shorter wavelength transitions. This is because the photocurrent is proportional to the product of the absorption strength and the probability of extracting the photogenerated carriers. For both QD samples, the ground states are deep in the potential well formed by the conduction and valence band edges of the surrounding matrix (GaAs for the conventional QDs and AlGaAs fence/GaAs for the DFENCE sample). The carrier extraction requires either tunneling through the barrier (assisted by the internal diode electric field) or thermionic emission over the top of the barrier. Both of these processes become less probable the deeper the states are below the barrier edge. This explains the general increase in the magnitude of the photocurrent with decreasing wavelength because it is due to absorption involving excited QD states that are closer in energy to the top of the barrier. The prominent feature near 900 nm in the standard QD is most likely associated with highest excited state (seen in Fig. 2 as a small feature in the PL spectrum) from which the carriers are most easily extracted. The overall suppression of the photocurrent for the DFENCE structure at all wavelengths beyond 900 nm and in particular in the wavelength region associated with the highest excited state (that was of comparable magnitude to the standard QD in the PL spectra) indicates that the AlGaAs fence layers are impeding the extraction of photogenerated carriers, not enhancing it as was theoretically predicted.<sup>8</sup> The fact that the magnitude of the photocurrent for both QD samples at wavelengths shorter

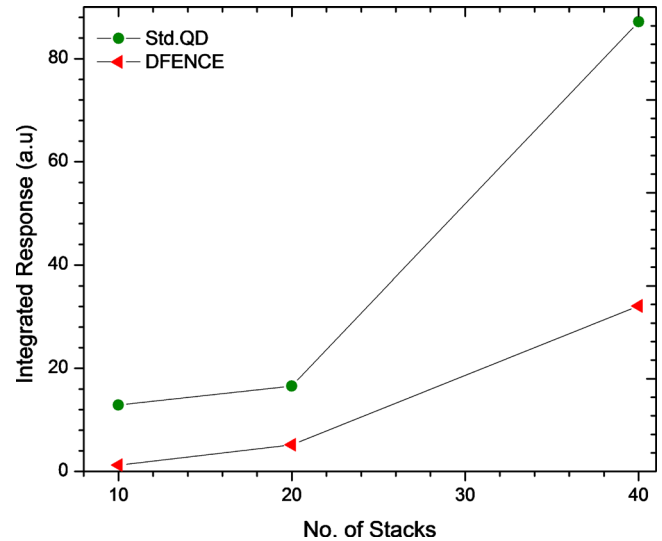


FIG. 4. (Color online) Photoresponse of the two QD sample types integrated over the wavelength region greater than 900 nm as a function of the number of dot layers.

than the GaAs band edge are comparable to the GaAs reference samples indicates that the QDs and the AlGaAs layers do not significantly affect the general carrier transport in the devices but it also indicates that there is no enhancement to the offdot transport as predicted theoretically.<sup>8</sup>

Figure 4 shows the photoresponse as a function of the number of dot layers for the two QD samples, integrated over wavelengths greater than 900 nm. The standard QD sample clearly generates more photoresponse than the DFENCE sample. The highly nonlinear dependence of the integrated response on number of dot layers is the result of the simultaneous increase in absorption and decrease in the built-in-field-assisted carrier extraction with increasing layer number.

## VI. SOLAR CELL PARAMETER DETERMINATION

Figures 5(a)–5(c) show the I–V characteristics measured under standard terrestrial illumination conditions (AM 1.5G at 100 mW/cm<sup>2</sup>) (Ref. 9) using a Newport Oriel PV calibrated solar simulator. The photocurrent was measured with an Agilent 4156C precision semiconductor parameter ana-

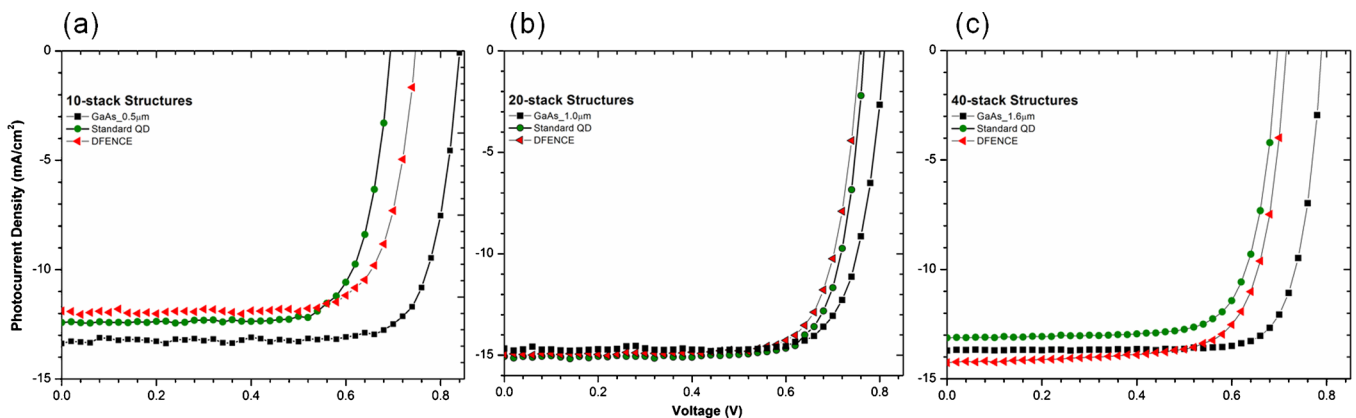


FIG. 5. (Color online) [(a)–(c)]. I–V characteristics of 10, 20, and 40 stack QD solar cells with and without an AlGaAs energy fence barrier layer and a corresponding 0.5, 1.0, and 1.6  $\mu\text{m}$  GaAs reference cell under AM 1.5G at 100 mW/cm<sup>2</sup>

TABLE I. Calculated short circuit current densities ( $J_{sc}$ ), open circuit voltages ( $V_{oc}$ ), FFs and efficiencies of the GaAs reference, conventional QD, and DFENCE test cells under AM 1.5G at an irradiance of 100 mW/cm<sup>2</sup>.

Stacks	$J_{sc}$ (mA/cm <sup>2</sup> )			$V_{oc}$ (V)			FF (%)			Efficiency (%)		
	GaAs	Std. QD	DFENCE	GaAs	Std. QD	DFENCE	GaAs	Std. QD	DFENCE	GaAs	Std. QD	DFENCE
10	13.38	12.42	11.89	0.84	0.71	0.75	77	75	75	9.1	6.8	6.9
20	14.66	15.07	14.97	0.81	0.77	0.75	79	77	77	9.8	9.3	8.9
40	13.74	13.17	14.31	0.79	0.69	0.71	80	76	75	8.7	6.9	7.5

lyzer. It is important to note that the dependence of the photocurrent under solar illumination conditions on the active region thickness is expected to be substantially different from the dependence shown in Fig. 3 since the majority of the spectral intensity is in the shorter wavelength region for which the absorption coefficient of GaAs is very high. This light will be efficiently absorbed in a thin layer near the surface, and does not penetrate into the thicker layers.

Solar cell parameters such as the short circuit current density ( $J_{sc}$ , the value of the photocurrent density at zero-bias), the open circuit voltage ( $V_{oc}$ , the voltage for which the net current is zero), the fill factor (FF, the ratio of the maximum obtained power and the product of the closed circuit current and  $V_{oc}$ ), and the external cell efficiency (the maximum power divided by the solar power incident on the cell) can be obtained from these curves. Table I gives a summary of the cell parameters for each of the samples.

The most obvious feature of the data shown in Fig. 5 is that for both QD sample types,  $V_{oc}$  is less than for the equivalent GaAs control sample.  $V_{oc}$  depends on, among other things, the band gap energy of the semiconductor and on carrier recombination in the material.<sup>9</sup> Some of the drop in  $V_{oc}$  could be attributed to the introduction of QDs that have a lower band gap than the GaAs host (which was intentionally done to capture more of the NIR spectrum). However, Fig. 5(a) shows that the DFENCE structure has a higher  $V_{oc}$  than the standard QD sample even though PL measurements showed that it had a slightly lower band gap. The higher  $V_{oc}$  is consistent with the predicted reduction in recombination (higher transmission through the offdot wetting layer) due to the presence of the AlGaAs barriers<sup>8</sup> but the trend is not well established in the other two sets of samples [Figs. 5(b) and 5(c)]. The slight reduction in  $J_{sc}$  for the 10 stack DFENCE sample compared with the standard QD sample [Fig. 5(a)] is consistent with the reduced integrated NIR photocurrent (Fig. 4), but, again, the other two sample sets do not support this explanation. The behavior of both  $V_{oc}$  and  $J_{sc}$  with different numbers of QD layers is most likely due to the complex interaction between the absorption strength, the carrier extraction, and the recombination in the dots and the wetting layer. A quantitative description of this dependence is beyond the scope of this work.

Figure 5 and Table I show that for all sample types (QDs and reference), the highest performance is obtained for the 20 stack QDs and the equivalent reference sample. The  $V_{oc}$  for the standard QD sample and the DFENCE sample are nearly the same and only slightly lower than for the reference

sample. The  $J_{sc}$  is virtually the same for all three sample types. This indicates that the presence of the QD layers is not introducing significant recombination of photogenerated carriers, but the QD samples do not show an enhancement over the performance of the reference sample due to either longer wavelength absorption or improved transport properties.

## VII. SUMMARY AND CONCLUSIONS

We have studied the effects of AlGaAs energy barrier fence layers surrounding self-assembled InAs QDs in a GaAs matrix on the properties of solar cell samples by comparing a series of samples with different numbers of dot layers with equivalent standard QD samples and GaAs reference samples. We have found that for the set of layer thicknesses chosen for this study, the primary effect of the energy fence is to suppress the extraction of carriers generated by photons with wavelengths longer than the cutoff wavelength of the GaAs matrix material. The absorption of longer wavelength radiation was found to have little effect on the performance of the cells. The presence of the dots in the matrix was found to have little detrimental effect on the performance of the cells, and an optimum number of layers was determined which maximized the cell parameters for the QD samples and the equivalent reference sample.

<sup>1</sup>A. Luque, A. Martí, C. Stanley, N. López, L. Cuadra, D. Zhou, J. L. Pearson, and A. McKee, *J. Appl. Phys.* **96**, 903 (2004).

<sup>2</sup>A. G. Norman, M. C. Hanna, P. Dippo, D. H. Levi, R. C. Reedy, J. S. Ward, and M. M. Al-Jassim, Proceedings of the 31st IEEE Photovoltaic Specialist Conference, Lake Buena Vista, FL, 3–7 January, 2005 (IEEE, New York, 2005), pp. 43–48.

<sup>3</sup>L. Cuadra, A. Martí, N. Lopez, and A. Luque, Proceedings of the 19th European Photovoltaic Solar Energy Conference, Munich, Germany, 7–11 June, 2004 (WIP, Munich, 2004), pp. 250–253.

<sup>4</sup>R. B. Laghumavarapu, M. El-Emawy, N. Nuntawong, A. Moscho, L. F. Lester, and D. L. Huffaker, *Appl. Phys. Lett.* **91**, 243115 (2007).

<sup>5</sup>R. B. Laghumavarapu, A. Moscho, A. Khoshakhlagh, M. El-Emawy, N. Nuntawong, L. F. Lester, and D. L. Huffaker, *Appl. Phys. Lett.* **90**, 173125 (2007).

<sup>6</sup>N. López, A. Martí, A. Luque, C. Stanley, C. Farmer, and P. Diaz, *ASME J. Sol. Energy Eng.* **129**, 319 (2007).

<sup>7</sup>M. Paxman, J. Nelson, B. Braun, J. Connolly, K. W. J. Barnham, C. T. Foxon, and J. S. Roberts, *J. Appl. Phys.* **74**, 614 (1993).

<sup>8</sup>G. Wei and S. R. Forrest, *Nano Lett.* **7**, 218 (2007).

<sup>9</sup>P. Baruch, A. De Vos, P. T. Landsberg, and J. E. Parrott, *Sol. Energy Mater. Sol. Cells* **36**, 201 (1995).

<sup>10</sup>P. Colí and G. Ianncone, *Nanotechnology* **13**, 263 (2002).

<sup>11</sup>D. S. Sizov, Y. B. Samsonenko, G. E. Tsyrlin, N. K. Polyakov, V. A. Egorov, A. A. Tonkikh, A. E. Zhukov, S. S. Mikhlin, A. P. Vasil'ev, Y. G. Musikhin, A. F. Tsatsul'nikov, V. M. Ustinov, and N. N. Ledentsov, *Semiconductors* **37**, 559 (2003).

<sup>12</sup>M. Arzberger, U. Kasberger, G. Bohm, and G. Abstreiter, *Appl. Phys. Lett.* **75**, 3968 (1999).